Electron acceleration from the breaking of relativistic plasma waves

A. Modena*, Z. Najmudin*, A. E. Dangor*, C. E. Clayton†, K. A. Marsh†, C. Joshi†, V. Malka‡, C. B. Darrow§, C. Danson‖, D. Neely‖ & F. N. Walsh‖

* Imperial College, Blackett Laboratory, Prince Consort Road, London SW7 2AZ, UK
† University of California at Los Angeles, Los Angeles, California 90024, USA
‡ LULI, Ecole Polytechnique, Palaiseau, France
§ Lawrence Livermore National Laboratory, Livermore, California 94550, USA
‖ Rutherford Appleton Laboratory, Didcot, UK

ELECTRONS in a plasma undergo collective wave-like oscillations near the plasma frequency. These plasma waves can have a range of wavelengths and hence a range of phase velocities[1]. Of particular note are relativistic plasma waves[2,3], for which the phase velocity approaches the speed of light; the longitudinal electric field associated with such waves can be extremely large, and can be used to accelerate electrons (either injected externally or supplied by the plasma) to high energies over very short distances[2–4]. The maximum electric field, and hence maximum acceleration rate, that can be obtained in this way is determined by the maximum amplitude of oscillation that can be supported by the plasma[5–8]. When this limit is reached, the plasma wave is said to 'break'. Here we report observations of relativistic plasma waves driven to breaking point by the Raman forward-scattering instability[9,10] induced by short, high-intensity laser pulses. The onset of wave-breaking is indicated by a sudden increase in both the number and maximum energy (up to 44 MeV) of accelerated plasma electrons, as well as by the loss of coherence of laser light scattered from the plasma wave.

The maximum amplitude of a plasma oscillation can be obtained from nonlinear plasma theory. As the wave grows, its waveform is no longer sinusoidal, that is, it steepens. In the cold-plasma theory[5,7], wave-breaking occurs when this steepening is so extreme that there are singularities in the plasma density. In reality, thermal effects determine the wave-breaking amplitude[6,8] for two reasons. First, the tendency of the plasma density to increase to infinity at the wave crests is opposed by plasma pressure, and second, at some large amplitude, plasma electrons with large thermal velocities along the direction of the phase velocity begin to be trapped and accelerated by the wave. A self-trapped electron is one that already has or picks up enough energy from the electric field of the wave to begin to move forward in the frame of the wave (to accelerate). Untrapped electrons simply move with their thermal velocity in addition to taking part in the coherent wave oscillations. At wave-breaking, the number of electrons being trapped is so large that these accelerating particles damp the wave irreversibly. As estimate of the maximum electric field for a relativistic plasma wave based on Gauss's law[11] gives $E = 0.96\alpha(n_e)^{1/2}$ V cm^{-1} where n_e is the plasma density in cm^{-3}, and $\alpha = \tilde{n}/n_e$ is the normalized density perturbation or wave amplitude and is ~1 at wave-breaking in our typical conditions, and $\tilde{n}$ is the magnitude of the perturbation of the electron density associated with the wave. Neglecting any beam loading effects, the maximum amount of energy[3,11] a trapped electron can obtain in such a wave is 'dephasing limited' to roughly $2\alpha\gamma_\phi^2 mc^2$ where $\gamma_\phi = (1 - v_\phi^2/c^2)^{-1/2}$ is the relativistic Lorentz factor associated with the phase velocity v_ϕ of the wave and m is the electron mass. Dephasing occurs when the accelerated electrons outrun the wave, limiting the useful interaction length. Observation of a sudden increase in both the number of self-trapped electrons accelerated by the plasma and maximum electron energy close to the dephasing-limited value is a strong indication that wave-breaking has occurred.

In the experiments described here, the relativistic plasma wave is excited by an intense ($> 5 \times 10^{18}$ W cm^{-8}), short-duration (< 1 ps), 1.054-μm-wavelength laser pulse via the Raman forward-scattering (RFS) instability[9,10]. This is the decay (induced by a noise-level plasma wave) of the strong electromagnetic pump wave (ω_o, k_o) into a plasma wave (ω_p, k_p) and two forward-propagating electromagnetic cascades at the Stokes ($\omega_o - n\omega_p$) and anti-Stokes ($\omega_o + n\omega_p$) frequencies. Here $\omega_p = (4\pi n_e e^2/m)^{1/2}$ is the plasma frequency, n is a positive integer, e is the electron charge, and w and k are the angular frequency and the wavenumber respectively, of the indicated waves. The spatial and temporal interference of these sidebands with the laser produces an electromagnetic beat pattern propagating synchronously with the plasma wave. The electromagnetic beat exerts a force on the plasma electrons, reinforcing the original noise-level plasma wave which then scatters more sidebands, thus closing the feedback loop for the instability[9].

The early experimental work on RFS was performed using long laser pulses (0.1–2 ns) of substantially lower intensity ($< 10^{15}$ W cm^{-2})[12–14]. In these experiments, the RFS instability was in the spatial-convective (long-pulse) regime. Although self-trapped electrons were observed out to 1.4 MeV in one of these experiments[12], the possibility of driving the plasma wave to its maximum wave-breaking level in all three of these experiments was precluded by the low laser intensities and the short interaction lengths. More recent experimental work on RFS involved the newer, short-pulse laser technology but still with relatively low intensity[15,16]. Acceleration of injected electrons was reported by Nakajima *et al.*[15] and correlation of accelerated electrons with an anti-Stokes sideband was reported by Coverdale *et al.*[16]. In neither case did plasma waves grow to wave-breaking as evidenced by the absence of copious electrons near the theoretical maximum energy. Finally, an experimental study of wavebreaking of non-relativistic plasma waves induced by Raman backscatter[9] was recently reported[17]. The main diagnostic, scattered light from an external probe beam, indicated destruction of the wave's coherence and trapping and acceleration of background electrons (up to 4 v_ϕ or ~1 keV) was inferred by computer simulations.

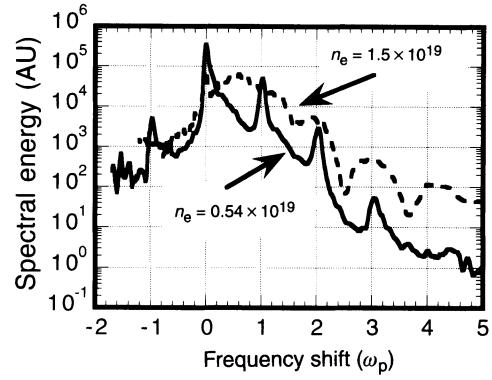

FIG. 1 Frequency spectrum of the light trasmitted through the plasma in the f/5 cone angle of the focused laser beam for two different plasma densities: 0.54×10^{19} cm^{-3} (solid curve) and 1.5×10^{19} cm^{-3} (dashed curve); AU, arbitrary units. Because the frequency scale has been normalized to ω_p, the sidebands have integer values for both densities. The spectrum was read out with a 16-bit silicon CCD camera which has essentially no sensitivity at wavelengths >1.2 μm. A bright blackbody source placed in the plasma location was used to measure the overall transmission function of the optics and the spectral response of the CCD camera, and this was used to correct the measured spectrum. The first Stokes sideband (at $\Delta\omega/\omega_p = -1$) in the low-density shot is just within the spectral sensitivity of the CCD camera, whereas the first Stokes sideband in the high-density shot is outside this sensitivity.

Other laser-driven plasma accelerators, namely the Plasma Wakefield Accelerator[3,18] (PWFA) and the Plasma Beat Wave Accelerator[3,4] (PBWA), have been discussed in the literature in the context of a future alternative technology to radio-frequency linear accelerators (linacs)[19]. In these schemes, wave-breaking is undesirable for issues relating to the beam quality of the output electron beam. Instead, a high-quality electron beam is injected into the plasma wave which is driven in a controlled manner by either a two-frequency laser beam (PBWA) or an extremely short (shorter than a plasma wavelength) laser pulse (PWFA) rather than through an instability of an intense, short (but longer than a plasma wavelength) laser pulse as is the case here. Recent experiments have reported an energy gain of about 13 MeV in the PWFA[15] and gains in 10–30 MeV range in the PBWA[20–23].

When a sufficiently intense short-pulse laser drives the RFS instability, the instability is said to be in the spatio-temporal regime. In this case, the plasma wave grows substantially in the frame of the laser pulse as the pulse transits the plasma. This is in contrast to the long-pulse, low-intensity laser case where the plasma wave growth is small on the scale of a plasma-transit time (for typical plasma lengths). The spatio-temporal theory of RFS for short pulses predicts[10] that the total gain G for the relativistic plasma wave growing from noise is given by $G = e^g/(2\pi g)^{1/2}$ where $g = [a_0/\sqrt{2}(1+a_0^2/2)](\omega_p/\omega_0)^2(\omega_0/c)\sqrt{x\psi}$. Here, $a_o = eA/mc^2$ is the normalized vector potential of the laser which is proportional to the square root of the laser intensity, x is the distance travelled into the plasma, and ψ/c is the length of time that the assumed constant-intensity pulse has interacted with the plasma at position, and A is the laser vector potential. To reach wave-breaking, that is $\alpha \approx 1$, we must have $G\alpha_n \approx 1$ where α_n is the initial noise level. Calculating this noise level for the general case is not possible because there are various complex mechanisms for generating the noise. For $n_e = 1.5 \times 10^{19}$ cm^{-3} and $a_o \approx 1$, the coupling between the laser and faster-growing (relative to RFS) but non-forward Raman scattering modes can be very strong and actually deplete a portion of the pump by scattering it into various angles[16,24,25]. Simulations show that this pump depletion can be quite localized on the rising edge ($a_o < 1$) of the pump and thus form a 'notch' on the pulse envelope after propagating only a fraction of Rayleigh length (the length over which a focused laser beam drops by a fraction of two in intensity) into the plasma[24,25]. The plasma wave 'wake' associated with this notch moves with the laser and therefore will act as an enhanced noise level to seed the RFS instability[24,25]. Because the instability growth rate g is weakly dependent on laser intensity for $1 < a_o < 2$, we can take the interaction time $\psi/c \approx 800$ fs (the duration of the pulse for which $a_o > 1$ at $x = 350$ μm). These parameters, along with a density of $n_e = 1.5 \times 10^{19}$ cm^{-3}, are sufficient to reach the wave-breaking condition $\alpha_n G \approx 1$ by the end of the pulse if $\alpha_n > 3 \times 10^{-5}$. Computer particle-simulations of this particular experiment[25] show that the noise level can be much greater than this value due to the above-described notching mechanism, leading to wave-breaking of RFS within a Rayleigh length for a smaller ϕ/c. Note that G is an extremely sensitive function of the electron density because g is proportional to n_e.

We report the results of an experiment where evidence for plasma wave-breaking has been observed using the VULCAN laser at Rutherford Appleton Laboratory[26] which provided 25-TW, 0.8-ps pulses on target with a 20-μm-diameter laser spot using $f/5$ optics. The effective Rayleigh length was 350 μm. The laser was focused onto the well-defined edge of a 4-mm-diameter, laminar plume of helium gas from a pulsed, supersonic gas jet[27] located 2 mm below the focal region. The maximum intensity of 6×10^{18} W cm^{-2} is sufficient to doubly-ionize the helium gas producing a fully-ionized plasma over at least 2 mm into the jet. The exponentiation rate $\ln(G(\phi, x))$ of the Raman instability, and therefore of the electron plasma wave, is approximately proportional to n_e. The plasma density was experimentally controlled by varying the backing pressure of the jet and was measured (through the frequency shift of the anti-Stoke sidebands) to be linear with backing pressure from 5 bar to at least 18 bar where the electron density was 1.5×10^{19} cm^{-3}. We expect that varying the density over this factor of ~3 should result in enormous changes in the final electron plasma wave amplitude. The two important diagnostics discussed here are the forward scattered electromagnetic spectra in the full $f/5$ for the incident laser cone and the energy spectra of trapped and accelerated electrons in an $f/60$ cone centred on the laser axis.

The solid curve in Fig. 1 shows the electromagnetic frequency spectrum emerging from the plasma with a density of 5.4×10^{18} cm^{-3} where the abscissa is the shift in frequency $\Delta\omega$ of the forward scattered light from the laser frequency in units of ω_p. The upshifted anti-Stokes and downshifted Stokes signals at $\Delta\omega/\omega_p = \pm 1$ are clearly visible as is the transmitted pump at $\Delta\omega/\omega_p = 0$ and the second and third anti-Stokes sidebands. These signals are sharply peaked, and their width indicates that the plasma wave which generated these signals must have a coherence time of the order of the laser pulse. The dashed curve in Fig. 1 shows the spectrum when the plasma density is increased to 1.5×10^{19} cm^{-3}. The most startling feature is the tremendous broadening of the individual anti-Stokes peaks at this higher density. This broadening is thought to be characteristic of wave-breaking and is mainly caused by the loss of coherence due to severe amplitude and phase modulation as the wave breaks. As wave-breaking evolves, the laser light no longer scatters off a collective mode of the plasma but instead scatters

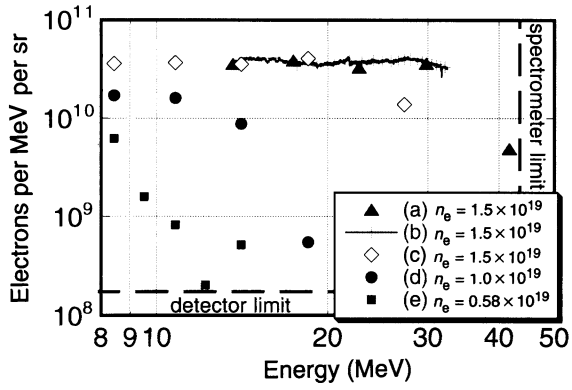

FIG. 2 The electron energy spectrum measured using a magnetic spectrometer in the forward $f/60$ cone centred on the laser axis for three different plasma densities: 1.5×10^{19} cm^{-3} (a–c), 1.0×10^{19} cm^{-3} (d) and 0.54×10^{19} cm^{-3} (e). All three cases were at a laser power of ~25 TW. Curves a and b were taken on the same laser shot with the highest magnetic field available in the spectrometer, whereas curve c was taken on a separate shot at a lower field strength. The variance between the two shots between 27 and 30 MeV may be indicative of the shot-to-shot reproducibility of the data. All the data except for curve b were taken with biased silicon surface-barrier detectors. Curve b was obtained using a fluorescer/film combination, giving a continuous spectrum from 13 to 32 MeV. For this film data, the vertical scale was adjusted to overlay the solid triangles for the same shot. The absolute electron flux was estimated from the known energy deposition rate (one electron–hole pair per 3.6 eV) in the silicon detectors along with the known sensitivity (volts per coulomb) in the preamplifiers. The energy plane dispersion (cm MeV^{-1}) was used to convert the signal on the 0.7-cm-wide detectors (signal per cm) into signal per MeV and thus electrons per MeV. Finally, the points were normalized to the $f/60$ solid angle (electrons per MeV per sr) to facilitate comparison of these electron spectra to spectral data in the literature. A peculiar aspect of the measured spectrum at high density is that it is approximately flat from 15 to 30 MeV. This is due to the fact that the observation is made in only an $f/60$ cone in the exact forward direction. The highest energy electrons are those that traverse the wave in the region of the highest longitudinal fields, that is, right down the axis of the plasma wave. Lower-energy electrons necessarily experience more of the radial fields and would tend to have a larger angular spread as a result.

individually off the trapped electrons which are still periodically deployed in space (that is, still k-matched to forward scattering) but having a range of momenta producing, therefore, a range of scattered frequencies[17]. Also, the Doppler shifts[28] expected for electrons moving at, say, a relativistic $\gamma \approx 4$ within a range of angles corresponding to $f/5$ focusing is approximately ω_p and nearly symmetric on the red and blue sides of the satellites which could further explain the 'filling in' of the satellites.

Figure 2 shows the measured electron energy spectra corresponding to the two optical spectra in Fig. 1 plus an intermediate plasma density of $1.0 \times 10^{19}\,\mathrm{cm}^{-3}$. The number of accelerated electrons at a given energy and the maximum electron energy both show a dramatic increase as the plasma density is increased to $1.5 \times 10^{19}\,\mathrm{cm}^{-3}$: the number of electrons above 20 MeV increases by at least two orders of magnitude and the accelerated electron distribution is rather flat up to 30 MeV where it begins to decrease with energy up to 44 MeV, which is the spectrometer limit. We interpret this sudden increase in accelerated electrons and maximum energy, together with the broadening of the electromagnetic spectrum, as the signature that wave-breaking has occurred. The large increase in the number of electrons accelerated at the highest plasma density is consistent with the wave trapping the bulk of the plasma thermal distribution function rather than a few tail particles at low plasma densities. Indeed the (spectrometer-limited) maximum electron energy of 44 MeV is not too far from the absolute maximum of 70 MeV that a test electron would obtain, limited by dephasing in an ideal plasma wave with $\alpha = 1$ which is near the relativistic warm-plasma wave-breaking limit expected for our plasma conditions.

We note that the normalized transverse emittance $\varepsilon_n = \gamma\sigma\delta\theta$ of any particular energy group from this experiment is quite small. Here γ is the relativistic Lorentz factor for that energy group, σ is the source size ($\sim$10 μm), and $\delta\theta$ the angular spread ($\sim$8 mrad due to the $f/60$ collection). At 30 MeV, $\varepsilon_n = 5\pi$ mm mrad which is low enough to be competitive with modern photoinjector-based linacs[29]. However, the beam current measured here ($\sim$1 A in a $\pm 1\%$ bandwidth around 30 MeV) is roughly 10–100 times lower than present-day photoinjector technology. The tremendous advantage over conventional linacs is the extremely short distance over which this energy is obtained. As dephasing limits the acceleration length to $\pi\gamma_\phi^3/k_0 \approx 300$ μm, the 44 MeV that the electrons gain indicate a peak electric field of over 100 GV m^{-1} which would represent the higher collective wave field ever produced in a laboratory. Given that laser technology, including repetition rate, average power, efficiency and smaller packaging is advancing very rapidly, it is reasonable to expect that the average current can be increased through a combination of higher laser frequencies and plasma densities as well as by increased repetition rate. Thus, one could envisage in the not-too-distant future a new class of compact accelerators based on the breaking of relativistic electron plasma waves which may find applications where 2–200 MeV electrons or photons are needed. □

Received 15 May; accepted 19 September 1995.

1. Stix, T. H. *The Theory of Plasma Waves* (McGraw-Hill, New York, 1962).
2. Dawson, J. M. *Scient. Am.* **260,** 54–61 (1989).
3. Tajima, T. & Dawson, J. M. *Phys. Rev. Lett.* **45,** 267–270 (1979).
4. Joshi, C. *et al. Nature* **311,** 525–529 (1984).
5. Dawson, J. M. *Phys. Rev.* **113,** 383–387 (1959).
6. Coffey, T. P. *Phys. Fluids* **14,** 1402–1406 (1971).
7. Akhiezer, A. I. & Polovin, R. V. *Sov. Phys. JETP* **3,** 696–699 (1956).
8. Katsouleas, T. & Mori, W. B. *Phys. Rev. Lett.* **61,** 90–93 (1988).
9. Forslund, D. W., Kindel, J. M. & Lindman, E. L. *Phys. Fluids* **18,** 1002–1016 (1975).
10. Mori, W. B., Decker, L. D., Hinkel, D. E. & Katsouleas, T. *Phys. Rev. Lett.* **72,** 1482–1485 (1994).
11. Chen, F. F. *Phys. Scripta* **T30,** 14–23 (1990).
12. Joshi, C., Tajima, T., Dawson, J. M., Baldis, H. A. & Ebrahim, N. A. *Phys. Rev. Lett.* **47,** 1285–1288 (1981).
13. Turner, R. E. *et al. Phys. Rev. Lett.* **57,** 1725–1728 (1986).
14. Batha, S. H. *et al. Phys. Rev. Lett.* **66,** 2324–2327 (1991).
15. Nakajima, K. *et al. Phys. Rev. Lett.* **74,** 4428–4431 (1995).
16. Coverdale, C. A. *et al. Phys. Rev. Lett.* **74,** 4659–4662 (1995).
17. Everett, M. J. *et al. Phys. Rev. Lett.* **74,** 1355–1358 (1995).
18. Sprangle, P., Esarey, E., Ting, A. & Joyce, G. *Appl. Phys. Lett.* **53,** 2146–2148 (1988).
19. Sessler, A. M. *Physics Today* **41,** 26–34 (1988).
20. Kitagawa, Y. *et al. Phys. Rev. Lett.* **68,** 48–51 (1992).
21. Clayton, C. E. *et al. Phys. Rev. Lett.* **70,** 37–40 (1993).
22. Everett, M. *et al. Nature* **368,** 527–529 (1994).
23. Ebrahim, N. A. *J. appl. Phys.* **76,** 7645–7647 (1994).
24. Decker, C. D., Mori, W. B. & Katsouleas, T. *Phys. Rev.* E**50,** R3338–R3341 (1994).
25. Tzeng, K-C., Mori, W. B. & Decker, C. D. *Phys. Rev. Lett.* (submitted).
26. Danson, C. N. *et al. Opt. Commun.* **103,** 392–397 (1993).
27. Brückner, R. thesis, Univ. Orléans (1994).
28. Jackson, J. D. *Classical Electrodynamics* (Wiley, New York, 1975).
29. Fraser, J. S. & Sheffield, R. L. *IEEE J. quant. Electr.* **23,** 1489–1496 (1987).

ACKNOWLEDGEMENTS. We thank C. Stenz and R. Brückner for the design of the gas jet nozzle. Our particular thanks are due to W. B. Mori for many discussions and K-C. Tzeng for access to unpublished PIC simulation results. This work was supported by the EPSRC, the EU and the US Department of Energy.

Modelling urban growth patterns

Hernán A. Makse*, Shlomo Havlin*† & H. Eugene Stanley*

* Center for Polymer Studies and Department of Physics, Boston University, Boston, Massachusetts 02215, USA
† Department of Physics, Bar-Ilan University, Ramat-Gan, Israel

CITIES grow in a way that might be expected to resemble the growth of two-dimensional aggregates of particles, and this has led to recent attempts[1–3] to model urban growth using ideas from the statistical physics of clusters. In particular, the model of diffusion-limited aggregation[4,5] (DLA) has been invoked to rationalize the apparently fractal nature of urban morphologies[1]. The DLA model predicts that there should exist only one large fractal cluster, which is almost perfectly screened from incoming 'development units' (representing, for example, people, capital or resources), so that almost all of the cluster growth takes place at the tips of the cluster's branches. Here we show that an alternative model, in which development units are correlated rather than being added to the cluster at random, is better able to reproduce the observed morphology of cities and the area distribution of sub-clusters ('towns') in an urban system, and can also describe urban growth dynamics. Our physical model, which corresponds to the correlated percolation model[6–8] in the presence of a density gradient[9], is motivated by the fact that in urban areas development attracts further development. The model offers the possibility of predicting the global properties (such as scaling behaviour) of urban morphologies.

In the model we now develop we take into account two points. First, data on the population density $\rho(r)$ of actual urban systems are known to conform to the relation[10] $\rho(r) = \rho_0 e^{-\lambda r}$, where r is the radial distance from the compact core, and λ is the density gradient. Therefore, in our model the development units are positioned with an occupancy probability $p(r) \equiv \rho(r)/\rho_0$ that behaves in the same fashion as is seen in observations of real cities. Second, in actual urban systems, the development units are not positioned at random. Rather, there exist correlations arising from the fact that when a development unit is located in a given place, the probability of adjacent development units increases; each site is not independently occupied by a development unit, but is occupied with a probability that depends on the occupancy of the neighbourhood.

In order to quantify these ideas, we use the correlated percolation model[6–8]. In the limit where correlations are so small as to be negligible[11,12], a site at position $\mathbf{r}$ is occupied if the occupancy variable $u(\mathbf{r})$—an uncorrelated random number—is smaller than the occupation probability $p(\mathbf{r})$. To introduce correlations among the variables, we convolute the uncorrelated variables $u(\mathbf{r})$ with a suitable power-law kernel[7], and define a new set of random variables $\eta(\mathbf{r})$ with long-range power-law correlations that decay as r^{-a}, where $r \equiv |\mathbf{r}|$. The assumption of power-law interactions is motivated by the fact that the 'decision' for a